JOC The Journal of Organic Chemistry

Article

pubs.acs.org/joc

Photoswitching of the Triplet Excited State of DiiodoBodipy-Dithienylethene Triads and Application in Photo-Controllable Triplet−Triplet Annihilation Upconversion

Jie Ma,[†] Xiaoneng Cui,[†] Fen Wang,[†,‡] Xueyan Wu,[†] Jianzhang Zhao,*[,†] and Xingwei Li*[,‡]

[†]State Key Laboratory of Fine Chemical, School of Chemical Engineering, Dalian University of Technology, Dalian 116024, People's Republic of China

[‡]Dalian Institute of Chemical Physics, Chinese Academy of Sciences, Dalian 116023, People's Republic of China

Supporting Information

ABSTRACT: Dithienylethene (DTE)-2,6-diiodoBodipy triads were prepared with the aim to photoswitch the triplet excited state of the 2,6-diiodoBodipy moiety. Bodipy was selected due to its low T_1 state energy level to avoid sensitized photocyclization of DTE, which is very often encountered in DTE photoswitches, so that the photochemistry of DTE and the organic chromophore can be addressed independently. This is the first time that DTE was covalently connected with an organic triplet photosensitizer. For the triad with DTE-o structure, selective photoexcitation into the diiodoBodipy part did not initiate photocyclization of DTE-o. Upon photoirradiation at 254 nm, thus the DTE-o → DTE-c transformation, the intersystem crossing (ISC) of 2,6-diiodoBodipy moiety was competed by the photoactivated resonance energy transfer (RET), with Bodipy as the intramolecular energy donor and DTE-c as energy acceptor. The fluorescence of Bodipy was quenched and the triplet state lifetime of Bodipy was reduced from 105.1 to 40.9 μs. The photoreversion is O_2-independent, but can be greatly accelerated upon selective photoexcitation into the diiodoBodipy absorption band (at 535 nm). We concluded that ISC is not outcompeted by RET. The photoswitching of the triplet state was transduced to the singlet oxygen photosensitizing, as well as triplet−triplet annihilation upconversion.

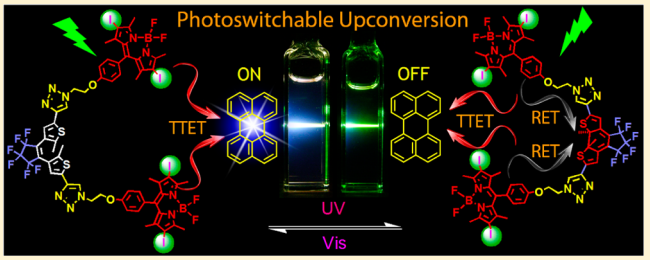

1. INTRODUCTION

Triplet excited states are important for photocatalysis, such as hydrogen (H_2) production by photocatalytic water splitting and photocatalytic organic reactions,[1−6] luminescent oxygen sensing,[7] molecular devices,[8,9] photodynamic therapeutic reagents,[10−13] and more recently the triplet−triplet annihilation (TTA) upconversion.[14−18] Concerning these applications, controllable production of triplet excited states by external stimuli will be a crucial progress, because this kind of switching ability will lead to versatile materials with spatial or temporal resolution, such as activatable photodynamic therapy (PDT) reagents,[9,10] molecular logic gates, etc.[8,9] However, the investigations on switching of triplet excited state are rarely reported.[19,20] As a result, the current knowledge on the photophysical processes regarding triplet state switching is limited.

Switching singlet excited state with external stimuli has been intensively investigated, and various mechanisms have been developed,[21] such as the photoinduced electron transfer (PET),[22] fluorescence resonance energy transfer (FRET or more precisely, RET),[23−25] through-band-energy-transfer (TBET),[26] etc. These mechanisms have been used to construct a lot of external stimuli-responsive molecules, such as fluorescent molecular sensors,[21] targeted luminescent bioimaging,[27−29] molecular beacons for detection of DNA, enzyme, or peptide,[30] light-harvesting molecular arrays,[24,31,32] and molecular logic gates.[33] Unfortunately, much room is left to extend the study to triplet excited-state switching. This situation can be attributed to a large extent to the difficulties to access organic triplet photosensitizers, for which the molecular design is still a substantial challenge.[2−4] Previously amino-containing bromo-aza Bodipy were studied as acid-activatable PDT reagents,[10] and the mechanism is based on PET. Molecular logic gates based on controlling of the direction of FRET were also studied, with acid-activated production of triplet excited state as a output of the logic gates.[8] These pioneering studies unveiled the fascinating area of triplet state switching or modulation. However, up to now such investigations are very rare, and we believe that more exemplars are needed to learn the photophysical principles governing the triplet excited-state switching. For example, the outcome of the parallel RET and intersystem crossing (ISC) processes in an organic dyad/triad was rarely studied; this competing process will be crucial for the modulation capability of the controlled production of triplet excited states.[9] Moreover, time-resolved transient absorption

Received: August 13, 2014
Published: October 23, 2014

   dx.doi.org/10.1021/jo5018662 | J. Org. Chem. 2014, 79, 10855−10866

Scheme 1. Preparation of DB-1 and DB-2[a]

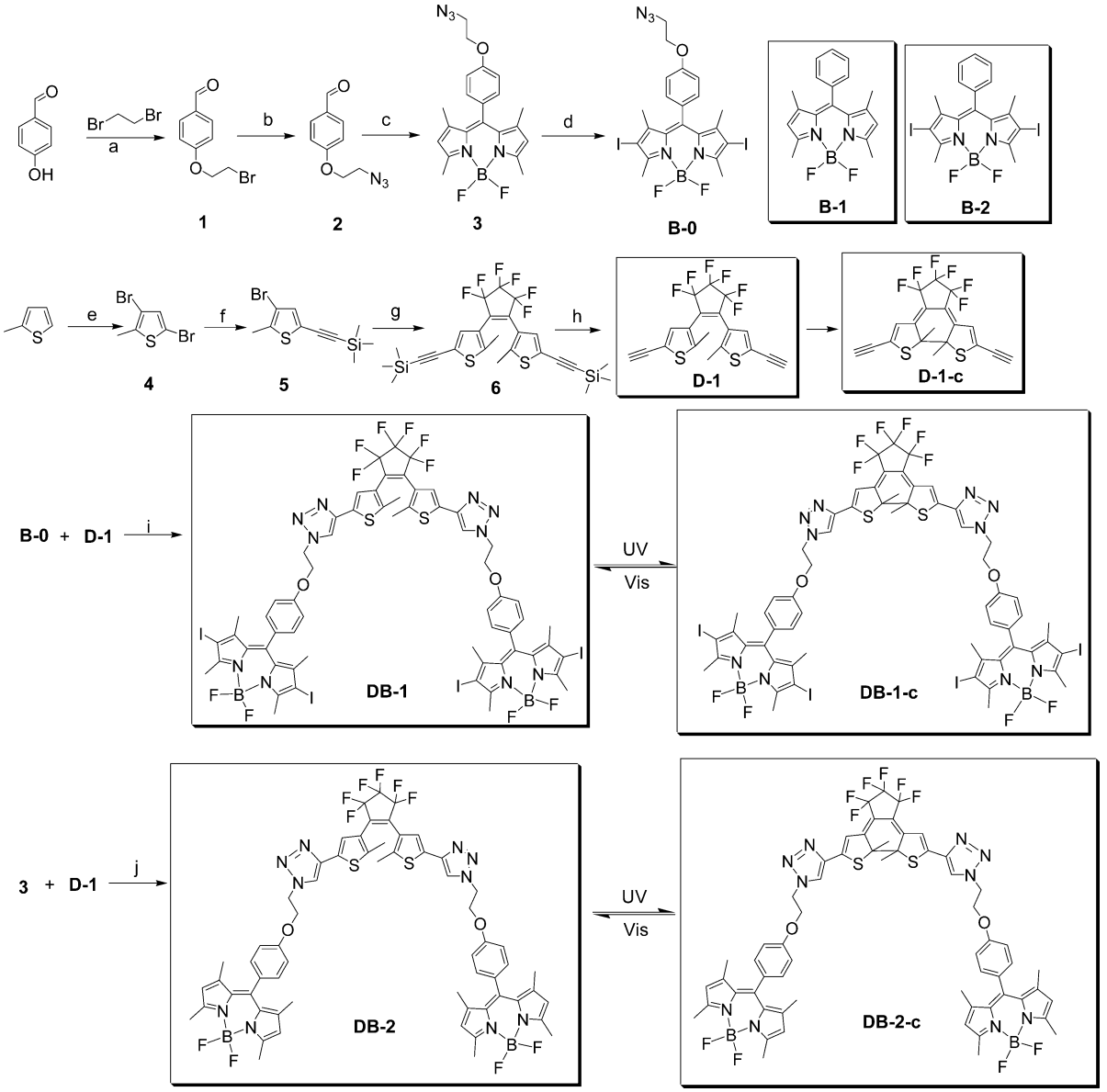

[a]Key: (a) K_2CO_3 and EtOH, reflux, 8 h, 60.0%; (b) NaN_3, DMF, 100 °C, 2 h, 80.4%; (c) N_2 atmosphere, 2,4-dimethylpyrrole, CH_2Cl_2, TFA; then DDQ, Et_3N, and $BF_3{\cdot}Et_2O$, 7.5%; (d) NIS, dry DCM, 30 °C, overnight, 90.4%; (e) NBS, AcOH, rt, overnight, 90.3%; (f) TMSA, $Pd(PPh_3)_4$, CuI, NEt_3, 45 °C, 7 h, 45.5%; (g) *n*-BuLi, perfluorocyclopentene, −78 °C, 4 h, 30.0%; (h) MeOH/THF, NaOH, 45 min, 70.0%; (i) sodium ascorbate, $CuSO_4$, 25 °C, Ar, 48 h, 46.6%; (j) sodium ascorbate, $CuSO_4$, 25 °C, Ar, 48 h, 73.4%.

spectroscopy, a powerful method for study of triplet excited state, was rarely used for detailed investigation of the triplet excited-state switching.[19]

On the other hand, dithienylethene (DTE) is of particular interest, due to its excellent photochromic property, such as the dramatic difference of absorption band position for the open-ring and the closed-ring isomers, and the thermal stability of open-ring and closed-ring isomers.[34−37] Previously, DTE or other photochromic units were used to switch the fluorescence property of Bodipy fluorophore.[38,39] DTE was also used for photoswitching of the triplet state of Ru(II) and Os(III) complexes,[19,40] Pt(II) acetylide complexes,[36b,41] Re(I) complexes,[42,43] or the intramolecular or intermolecular electron transfer,[44,45] but DTE was not used in any photoswitching of the triplet excited states of organic chromophores. Moreover, a long-standing challenge in the study of the photoswitching of the triplet state of the DTE−metal complex dyads is that the photocyclization of DTE is very often sensitized by excitation into the ^{1}MLCT band of the transition metal complexes,[19,36b,40−43,46] which makes it difficult to address the photochromic and the luminescent modules in the dyads independently. For example, it is difficult to achieve non-destructive readout of the luminescence or the triplet state property of the organic chromophore in the conventional DTE dyads. Recently, the photoswitching singlet oxygen production with porphyrin complexes by DTE was reported.[47a] We also studied the photoswitching of the TTA upconversion with two DTE compounds.[47b] However, the photoswitching is based on a mixture of the DTE derivatives and the triplet photosensitizer/acceptor. A covalently linked DTE-photosensitizer was never studied.

dx.doi.org/10.1021/jo5018662 | J. Org. Chem. 2014, 79, 10855−10866

To address the above challenges, herein we prepared an iodoBodipy-dithienylthene (DTE) triad for study of photoswitching of triplet excited states of organic chromophores (**DB-1**, Scheme 1). 2,6-DiiodoBodipy in **DB-1** is the triplet excited-state producer, or the spin converter.[4,48] DTE can be photoswitched from the open-ring form (DTE-o) to the closed-ring from (DTE-c), accompanied by substantial changes in UV−vis absorption wavelength (i.e., the S_1 state energy level) and triplet state energy levels.[19,40] Thus, the RET from iodo-Bodipy to the DTE-c will compete with the ISC of 2,6-diiodoBodipy moiety. As a result, the production of triplet excited state by iodo-Bodipy will be compromised upon photoirradiation. Steady-state and nanosecond time-resolved absorption and emission spectroscopy, as well as DFT computations, were used to study the photoswitching of triplet excited states. We found that the triplet excited-state lifetime, as well as the singlet oxygen ($^1O_2$) production capability of the triad can be significantly photoswitched. Furthermore, we found that the RET is unable to inhibit the ISC completely, which is different from a previous observation.[9] To the best of our knowledge, this is the first time that the triplet excited state of organic chromophores was used as a relay of the photochromic binary states' photoconversion. These studies will be useful for further exploration of the uncharted area of triplet excited-state switching, as well as for the application of the related switchable triplet photosensitizers in PDT, photocatalysis, upconversion, and molecular devices, etc.

2. RESULTS AND DISCUSSION

2.1. Molecular Design and Preparation of the Compounds. The rationale for designing of **DB-1** (Scheme 1) is to introduce a photoactivatable RET to compete with ISC; thus the production of triplet excited state may be photoswitched. Visible light-harvesting 2,6-diiodoBodipy was selected as the spin converter to produce the triplet excited state. Bodipy was selected as the chromophore due to its desired photophysical properties, such as strong absorption of visible light, high fluorescence quantum yields, good photostability, and feasible derivatization. DTE was selected as the photoswitchable unit.[49−52] The open-ring form of DTE (DTE-o) gives no visible light absorption, and the T_1 state energy level of DTE-o is presumably higher than the diiodoBodipy unit. Thus, the ability of diiodoBodipy unit to produce triplet excited state will not be reduced. Upon photoirradiation at 254 nm, the closed-ring form of DTE (DTE-c) will be produced, for which the absorption band moves to the visible spectra region (centered at 570 nm). Thus, there is a significant overlap between the emission of the Bodipy moiety and the absorption of the closed-ring form of DTE, and RET from the diiodoBodipy moiety, which shows fluorescence emission at 553 nm, to the closed-ring DTE moiety (λ_{abs} = 600 nm) may take place. As a result, the capability of the diiodoBodipy to produce triplet excited states may be compromised by the parallel RET effect.

Azide-diiodoBodipy (compounds **3** and **B-0**) was prepared as the key intermediate (Scheme 1). **D-1-c** is the ethynyl DTE. Cu(I)-catalyzed Click reaction gives the production of **DB-1**. **DB-2** was prepared as a reference compound. All of the new compounds were characterized with ^{1}H NMR, ^{13}C NMR, and HRMS. The compounds were obtained in moderate to satisfactory yields (see Experimental Section). The ^{1}H NMR spectrum of each of the DTE derivatives shows only a single set of signals, indicating that the compounds take antiparallel geometry or rapid interconversion of the two conformers occurs.[43] Recently, we studied the photoswitching of TTA upconversion with DTE derivatives, but that approach is based on the mixture of the three components.[47b] Herein, for the first time a covalently connected DTE-photosensitizer dyad/triad was studied for TTA upconversion. Different results were observed from the previous study.[47b]

2.2. UV−Vis Absorption and Fluorescence Emission Spectra. The UV−vis absorption spectra of the compounds were studied (Figure 1). **DB-1** shows a strong absorption band

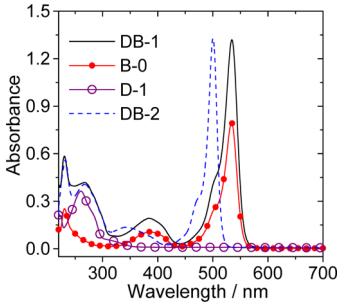

Figure 1. UV−vis absorption of **DB-1**, **DB-2**, **D-1**, and **B-0**. $c = 1.0 \times 10^{-5}$ M in CH_2Cl_2, 20 °C.

at 535 nm, which is due to the diiodoBodipy moiety. DTE gives no absorption in visible spectral region in its open-ring form, demonstrated by the absorption of the reference compound **D-1**. Without iodo atoms on the Bodipy moiety, **DB-2** gives slightly blue-shifted absorption band at 502 nm as compared to that of **DB-1**.[53] The absorption wavelength of **DB-1** (535 nm) is similar to that of **B-0**, and the molar absorption coefficient of **DB-1** is ca. 2-fold greater than that of **B-0**. On the basis of these results, we propose that there is no significant interaction between the DTE-o and the Bodipy moiety in **DB-1**.[38] Similar results were obtained for **DB-2**.

The photocyclization of the compounds upon irradiation was studied (Figure 2). Upon irradiation at 254 nm, the absorption band at 268 nm decreased, and a new broad absorption band at 600 nm developed (Figure 2a). This new absorption band is attributed to the DTE-c moiety.[38,54a] The DTE-o → DTE-c photocyclization is reversible; that is, upon photoirradiation at 600 nm, the new absorption band at 600 nm disappeared completely and the absorption band at 268 nm fully recovered (Figure 2b). The absorption band at 535 nm, due to the iodo-Bodipy moiety, did not change throughout the experiments, indicating the good photostability of the Bodipy moieties in **DB-1** and **DB-2**.[38] At the photostationary state (PSS) upon 254 nm photoirradiation, the conversion yield (open form → closed form) of **DB-1** and **DB-2** is 85.2% and 92.7%, respectively (based on HPLC, Supporting Information Figures S33, S34).

The quantum yields of the photocyclization and the photoreversion processes were studied with a chemical actinometer potassium ferrioxalate actinometer.[38] For **DB-1**, photocyclization quantum yield (open form → closed form) is $\Phi_{O\rightarrow C} = 0.32$; the photoreversion (closed form → open form) quantum yield is $\Phi_{C\rightarrow O} = 0.032$. For **DB-2**, the photocyclization (open form → closed form) quantum yield is $\Phi_{O\rightarrow C} = 0.37$; the photoreversion (closed form → open form) quantum yield is $\Phi_{C\rightarrow O} = 0.043$. These values are close to DTE derivatives without the Bodipy appendents.[47b]

dx.doi.org/10.1021/jo5018662 | J. Org. Chem. 2014, 79, 10855−10866

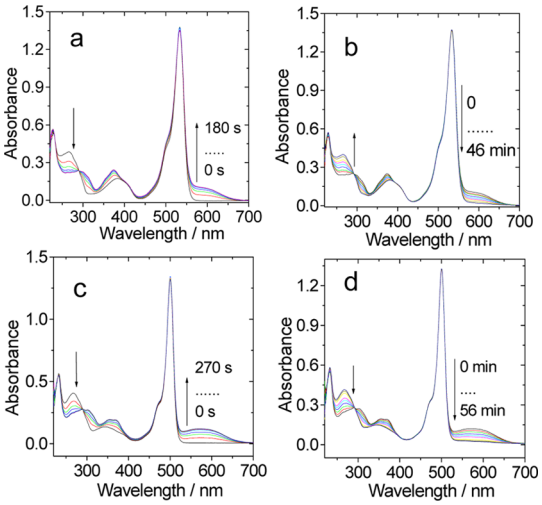

Figure 2. UV−vis absorption of **DB-1** upon irradiation. (a) Photoirradiation at λ_{ex} = 254 nm. After establishment of the photostationary state, then (b) photoirradiated at 600 nm (2.0−2.4 W/m^2). UV−vis absorption of **DB-2** and the absorption spectral changes upon irradiation at (c) λ_{ex} = 254 nm (0.7−1.0 W/m^2), and then with successive photoirradiation at (d) 570 nm (2.0−2.4 W/m^2). c = 1.0 × 10^{-5} M in CH_2Cl_2, 20 °C.

Interestingly, we found that by photoirradiation at 535 nm, where the diiodoBodipy moiety has a strong absorption, the conversion of DTE-c → DTE-o is greatly accelerated (Supporting Information Figure S23a), which is attributed to the RET from the Bodipy moiety to the DTE-c moiety. This observation is different from a previous study.[38] This trend is clearly demonstrated in Supporting Information Figure S24. Similar results were found for **DB-2** (Supporting Information Figure S23b).

The kinetics of the DTE-o ↔ DTE-c photoswitching (photocyclization and photocycloreversion) were studied (Supporting Information Figure S24). **DB-1**, **DB-2**, and **D-1** give similar DTE-o → DTE-c kinetics (Figure S24a). For example, the rate constants of the photocyclization reaction are 1.1 × 10^{-3}, 1.2 × 10^{-3}, and 9.0 × 10^{-4} s^{-1}, respectively. These results indicate that the DTE-o → DTE-c photocyclization is via singlet excited state, otherwise the T_1 state of the DTE-o will be quenched by the T_1 state of Bodipy, for which the T_1 state energy level is 1.52 eV, lower than that of DTE-o (1.97 eV). As a result, the photocyclization will be retarded.[19] Photostationary state was reached after 3 min of photoirradiation at 254 nm for **DB-1** (Supporting Information Figure S24a).

For the DTE-c → DTE-o transformation, generally the reaction rate constants are much smaller than the open-ring → closed-ring photocyclization reaction, which is similar to the reported DTE compounds.[42,43] The rate constants of the photoreversion are 5.33 × 10^{-5}, 5.33 × 10^{-5}, and 8.33 × 10^{-5} s^{-1} for **DB-1**, **DB-2**, and **D-1**, respectively. The reference compound **D-1** gives slightly faster kinetics (Supporting Information Figure S24b).

Our results show that the DTE-c → DTE-o process is faster with irradiation at the absorption band of the iodo-Bodipy and the Bodipy moiety. The results show that photoreversion DTE-c → DTE-o is not sensitive to the presence of O_2 in the solution. Thus, the T_1 state energy level of the DTE-c moiety is higher than the T_1 state energy level of the iodo-Bodipy moiety; thus the photoreversion can not be sensitized by iodo-Bodipy.[19] The studies on fluorescence confirmed this conclusion. The DTE-c → DTE-o takes place via a singlet excited state of DTE-c; otherwise the photoreaction will be inhibited in the presence of O_2.[19,41] Thus, we propose that singlet RET takes place with Bodipy/iodo-Bodipy as energy donor and DTE-c as energy acceptor. This is different from our previous study in that FRET was not involved in the photoswitching.[47b]

We also studied the possibility of the photosensitized DTE-o → DTE-c process upon selective excitation into the Bodipy moieties in **DB-1** (Supporting Information Figure S25). Upon photoirradiation at 535 nm, no absorption band at 600 nm was observed for **DB-1-o**. This result shows that the energy level of the T_1 state of the Bodipy is lower than that of **DTE-o**; thus, no sensitized photocyclization was observed. This observation is contrary to the previous report that in the Ru(II) or Os(III) complex, the DTE-o → DTE-c can be sensitized via the ^{3}MLCT state of the coordination center; as a result, the photophysical property of the visible light-absorbing chromophore cannot be addressed independently with the open form DTE.[19] For the current triads, however, both the singlet excited state and the triplet excited state of the Bodipy chromophore can be independently manifested, which may offer improved tuning capability of these molecular assemblies.

2.3. Switching of the Fluorescence Emission. The fluorescence switching effect of compounds **DB-1** and **DB-2** was also studied (Supporting Information Figure S26). For **DB-1**, the fluorescence of the diiodoBodipy unit decreased upon 254 nm photoirradiation, that is, the DTE-o → DTE-c photocyclization. This process is reversible, and the fluorescence emission intensity at 553 nm can be recovered upon 600 nm irradiation of the **DB-1-c**, via the DTE-c → DTE-o transformation (Supporting Information Figure S26b).

The switching of the fluorescence of **DB-2** was also studied (Supporting Information Figure S26c and S26d). The modulation efficiency on the fluorescence of **DB-2** is more significant than that of **DB-1**. For example, the fluorescence of **DB-1** decreased to 61.0% of the initial value, whereas for **DB-2**, the fluorescence reduced to 11.6% of the initial intensity. Considering the open form/closed form ratio at PSS, the FRET efficiency can be estimated as 45.8% and 95.4% for **DB-1** and **DB-2**, respectively.[39c] The plausible reason for the different modulation efficiency on the fluorescence for **DB-1** and **DB-2** may be the different lifetimes of the singlet excited state of the compounds. The singlet state lifetime of **DB-1** (τ_F = 0.31 ns) is much shorter than that of **DB-2** (τ_F = 4.24 ns). Thus, the parallel RET has more difficulty competing with a fast decaying S_1 state of Bodipy moiety in **DB-1-c** than that in **DB-2-c**. The shorter fluorescence lifetime of **DB-1-c** is due to the ISC of the diiodoBodipy moiety. Previously, we studied the photoswitching of TTA upconversion in the mixture of DTE derivative, triplet photosensitizers, and triplet acceptor.[47b] However, switching of the fluorescence of the triplet photosensitizer is impossible with this "supramolecular approach". Thus, the present covalent bonded triad offers a new modulability.

On the basis of the fluorescence quenching and the fluorescence lifetime of the 2,6-diiodoBodipy, the rate constants of the RET in **DB-1-c** were calculated with eq 1.[54b]

$$k_{EnT} = \left[\frac{\Phi_{PL(DiiodoBodipy)}}{\Phi_{PL(DB\text{-}1\text{-}c)}} - 1\right]/\tau_0 \quad (1)$$

dx.doi.org/10.1021/jo5018662 | J. Org. Chem. 2014, 79, 10855−10866

Table 1. Photophysical Properties of DB-1, DB-2, B-0, and D-1[a]

					Φ_Δ[h]/%		Φ[i]/%		τ[e]/ns	
compd	λ_{abs}[b] /nm	ε[c]	λ_{em}[d]/nm	τ_T[f] (μs)	open-ring	closed-ring	open-ring	closed-ring	open-ring	closed-ring
DB-1	535	1.32	553	105.1[k]/40.9[l]	87.6	36.9	3.0	1.6	0.31	–[g]
DB-2	502	1.25	515	–[j]	–[j]	–[j]	80.5	14.3	4.24	3.67
B-0	534	0.80	553	106.4	–[j]	–[m]	4.7	–[m]	0.32	–[m]
D-1	261	0.36	–[m]	–[j]	–[j]	–[m]	–[j]	–[m]	–[j]	–[m]

[a]The excitation wavelengths for **DB-1**, **DB-2**, and **B-0** were 510, 480, and 510 nm, respectively (1.0×10^{-5} M, 20 °C). [b]Absorption wavelength. [c]Molar extinction coefficient. ε: 10^5 M^{-1} cm^{-1}. In dichloromethane. [d]Fluorescence emission wavelength. [e]Fluorescence lifetimes. [f]Triplet state lifetimes. [g]Too weak to be determined accurately. [h]Quantum yield of singlet oxygen ($^1O_2$), with **B-2** as standard (Φ_Δ = 0.83), λ_{ex} = 500 nm. [i]Fluorescence quantum yields in DCM, **DB-1**, and **B-0** with **B-2** (0.027 in CH_3CN) as the standard, **DB-2** with **B-1** (0.72 in THF) as the standard. [j]Not determined. [k]Triplet state lifetimes of **DB-1-o** in deaerated CH_3CN. [l]Triplet state lifetimes of **DB-1-c** in deaerated CH_3CN. [m]Not applicable.

where k_{EnT} is the RET rate constant, $\Phi_{PL(DiiodoBodipy)}$ is the fluorescence quantum yield of 2,6-diiodoBodipy, $\Phi_{PL(DB\text{-}1\text{-}c)}$ is the fluorescence quantum yield of the iodoBodipy part in **DB-1-c**, and τ_0 is the fluorescence lifetime of diiodoBodipy. The k_{EnT} was calculated as 6.1×10^9 s^{-1}. Previously, it was reported that the intersystem crossing rate constant of a 2,6-diiodoBodipy derivative is 7.87×10^9 s^{-1}.[54c] Thus, the RET is unlikely to compete efficiently with the ISC of the 2,6-diiodoBodipy part; as a result, in **DB-1-c**, the population of the triplet state of the 2,6-diiodoBodipy part is still significant. This is in agreement with the nanosecond transient difference absorption spectral study (see later section), as well as the singlet oxygen production with **DB-1-c** (Figure 7 and Table 1).

To confirm the above explanation, the RET in **DB-2-c** was analyzed with eq 1. The k_{EnT} of **DB-2-c** was calculated as 1.1×10^9 s^{-1}. This value is slightly decreased as compared to that in **DB-1-c**, which is probably due to the less matched spectral overlap between the emission of Bodipy and the absorption of the **DTE-c** unit. The values obtained for **DB-1-c** and **DB-2-c** are very close to that obtained with a Bodipy-spiropyran dyads fluorescence switch.[39c] The fluorescence of the triads was compared to that of the reference compounds (Supporting Information Figure S27). For **DB-1-o**, the fluorescence intensity is close to that of **B-0** (the two solutions have the same optical density at the excitation wavelength) (Supporting Information Figure S27a). Therefore, it is plausible to assume that no significant photoinduced electron transfer exists in **DB-1-o**. Similar results were observed for **DB-2-o** (Supporting Information Figure S27b). The fluorescence emissions of **B-0**, **DB-1-o**, and **DB-1-c** were compared in solvents with different polaritie (see Supporting Information Figure S28). The emission intensity ratios of the three compounds are the same. Therefore, we conclude that no significant intramolecular electron transfer exists for the singlet excited state of the compounds. Similar results were observed for **DB-2** (see Supporting Information Figure S29).

2.4. Electrochemical Studies: Free Energy Changes of the Photoinduced Electron Transfer. For **DB-1-o**, an irreversible reductive wave was observed at −1.91 V (Figure 3a), which is assigned to **DTE-o** moiety.[43] The reversible reduction wave at −1.27 V can be attributed to the 2,6-diiodoBodipy moiety. An irreversible oxidation peak at +0.88 V is due to the diiodoBodipy moiety (Table 2). For the closed-form **DB-1-c**, two new irreversible reduction waves at −1.40 and −1.74 V (this value was not presented in Table 2) were observed, which is similar to a previously reported DTE−Re(I) complex.[43] A new pseudoreversible oxidation band at +0.55 V was observed, which can be assigned to the closed-ring form of DTE. Considering the fast ISC of the 2,6-diiodoBodipy, we assume the triplet excited state of the 2,6-diiodoBodipy will initiate the electron transfer process. However, the free energy change was calculated as +0.28 eV. Thus, the photoinduced intramolecular electron transfer is unlikely to occur. This postulation is in agreement with the luminescence studies.

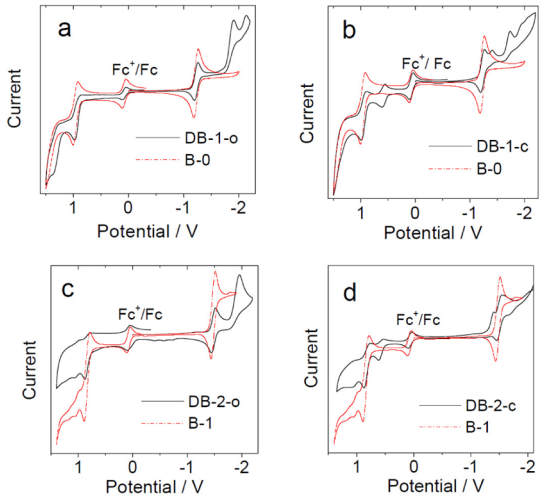

Figure 3. Cyclic voltammetry of (a) **B-0** ($c = 1.0 \times 10^{-3}$ M) and **DB-1-o** ($c = 5.0 \times 10^{-4}$ M); (b) **B-0** ($c = 1.0 \times 10^{-3}$ M) and **DB-1-c** ($c = 5 \times 10^{-4}$ M); (c) **B-1** ($c = 5.0 \times 10^{-4}$ M) and **DB-2-o** ($c = 1.0 \times 10^{-3}$ M), and (d) **B-1** ($c = 5.0 \times 10^{-4}$ M) and **DB-2-c** (1.0×10^{-3} M). In deaerated CH_3CN solutions containing 0.10 M Bu_4NPF_6 as supporting electrode, $Ag/AgNO_3$ reference electrode. Scan rate: 50 mV/s. Ferrocene (Fc) was used as internal reference 20 °C.

Table 2. Electrochemical Data for Compounds DB-1-o, DB-1-c, DB-2-o, DB-2-c, D-1-o, D-1-c, B-0, and B-1[a]

	E_{ox} (V)		E_{red} (V)	
compd	I	II	I	II
B-0	+0.96	–[b]	−1.23	–[b]
B-1	+0.84	–[b]	−1.48	–[b]
D-1-o	+0.35	–[b]	−1.15	–[b]
D-1-c	+0.87	–[b]	−1.19	−1.54
DB-1-o	+0.88	–[b]	−1.27	−1.91
DB-1-c	+0.55	+0.98	−1.27	−1.40
DB-2-o	+0.83	–[b]	−1.51	−1.96
DB-2-c	+0.54	+0.78	−1.38	−1.55

[a]Recorded with $[Bu_4N][PF_6]$ as the supporting electrolyte in deaerated CH_3CN (0.1 M) at ambient temperature with a scan rate of 50 mV/s. Potentials are expressed as the half-wave potentials ($E_{1/2}$) in volts vs $Ag/AgNO_3$ electrode using ferrocene as an internal reference. [b]Not applicable.

dx.doi.org/10.1021/jo5018662 | J. Org. Chem. 2014, 79, 10855−10866

2.5. Nanosecond Time-Resolved Transient Difference Absorption Spectra: Photoswitching of the Triplet Excited State. To study the photoswitching of the triplet excited states of the triads, nanosecond time-resolved transient difference absorption (TA) spectroscopy of the compounds was studied (Figure 4). First the TA of **DB-1-o** was studied

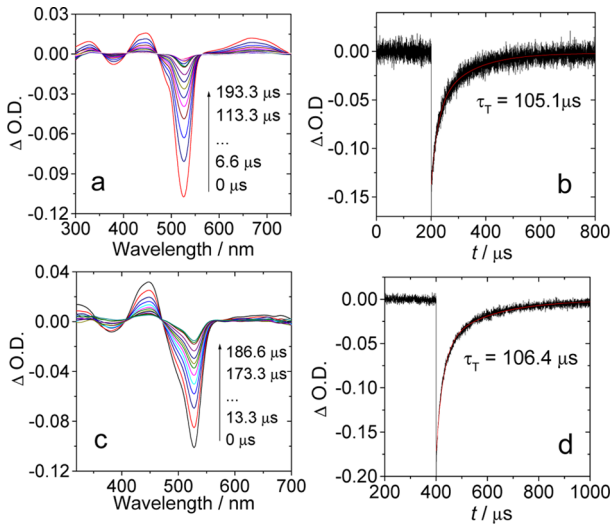

Figure 4. Nanosecond time-resolved transient difference absorption spectra. (a) **DB-1-o**. (b) Decay trace of **DB-1-o** at 530 nm. (c) TA spectra of **B-0**. (d) Decay trace of **B-0** at 530 nm. With pulsed laser excitation (λ_{ex} = 535 nm), $c = 1.0 \times 10^{-5}$ M in deaerated CH_3CN, 20 °C.

with 535 nm pulsed laser excitation. We have shown that no photocyclization reaction takes place upon excitation at this wavelength. This is actually a benefit to use chromophores showing long absorbing wavelength and lower T_1 state energy level than the **DTE-o** moiety; otherwise the sensitized photocyclization will take place and it will be difficult to observe the transient spectra of the visible light-harvesting chromophore.[19] Usually only the accumulation of the open-ring or the closed-ring photoproduct can be observed upon UV or visible light excitation, for example, in the DTE-containing Ru(II) complexes for which the photoreaction can be sensitized by the Ru(II) complex ^{3}MLCT state.[44]

Upon pulsed laser excitation at 535 nm, a bleaching band at 530 nm was observed for **DB-1-o**, together with transient absorption bands at 445 nm and in the region of 550−750 nm (Figure 4a). The lifetime of the triplet state was determined as 105.1 μs. These features are close to the results of the reference compounds **B-0** (Figure 4c and d). These results indicated that the energy level of the triplet state of 2,6-diiodoBodipy (1.52 eV)[55−58] is lower than that of DTE-o (1.97 eV).[19] As a result, the triplet state of the diiodoBodipy was not perturbed by the DTE-o moiety; that is, the DTE-o → DTE-c can not be sensitized by the selective excitation into the diiodoBodipy moiety, and therefore the triplet excited-state lifetime of **DB-1-o** is close to that of **B-0**. This result is different from the recent studies on the DTE−Ru(II) and DTE−Os(III) complexes, for which sensitized photocyclization always occurs and the triplet excited state of the Ru(II) coordination center is quenched.[19] Furthermore, the photoinduced electron transfer in **DB-1-o** is not significant; otherwise the triplet state lifetime of **DB-1-o** will be substantially shortened. This conclusion is also supported by the comparison of the fluorescence of **DB-1-o** and the reference compound **B-0** (Supporting Information Figure S27).

The TA spectrum of the **DB-1-c** was also studied (Figure 5). Because of the DTE-c → DTE-o transformation upon

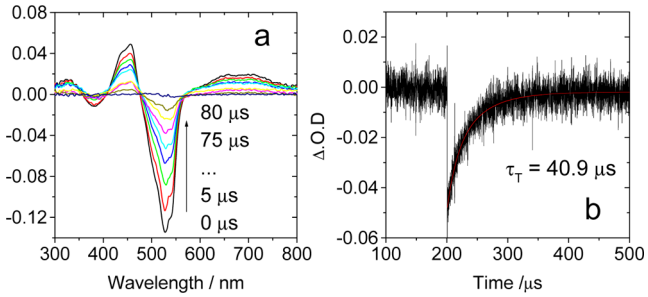

Figure 5. Nanosecond time-resolved transient difference absorption spectra of **DB-1-c**. (a) TA spectra after pulsed laser excitation (λ_{ex} = 532 nm, ICCD detector). (b) Decay trace at 530 nm (PMT detector). $c = 1.0 \times 10^{-5}$ M in deaerated CH_3CN, 20 °C.

photoexcitation at 535 nm, thus to reduce the photoreversion reaction, an ICCD detector (spectral mode) was used for the TA measurement to minimize the exposure of the **DB-1-c** solution to photoirradiation. Bleaching band at 528 nm was found, as well as the transient absorption band at 455 nm and the band in the region of 550−750 nm. These features are in agreement with that of the 2,6-diiodoBodipy (Figure 4c). The triplet state lifetime was determined as 40.9 μs, which is much shorter than that of **B-0** and **DB-1-o** (106.4 and 105.1 μs, respectively). Similar transient absorption spectra were obtained in DCM, for which longer lifetimes of the triplet exited state of **DB-1-o** (144.5 μs) and **DB-1-c** (42.3 μs) were observed (Supporting Information Figures S30 and S32). Since we have shown that photoinduced electron transfer is not significant for **DB-1-c**, thus the reduced triplet state lifetime is probably due to the intermolecular quenching effect of a the low-lying triplet state, such as the T_1 state of the DTE-c moiety. Note there exists a **DB-1-c** and **DB-1-o** equilibrium at the PSS. For the neat **DB-1-c**, the triplet state localized on diiodoBodipy may be quenched completely.[19a] It was reported that the lifetime of the ^{3}DTE-c is less than 10 ns,[19] which is beyond the response time of our nanosecond time-resolved transient absorption spectrometer. The energy level of this state is unknown. Furthermore, we have shown that RET is possible for **DB-1-c**; thus the parallel processes of RET and ISC take place. The quenched triplet state lifetime of the iodo-Bodipy moiety in **DB-1-c** and the reduced $^1O_2$ quantum yield of **DB-1-o** as compared to that of **B-0** support this conclusion.[19]

To study the localization of the triplet excited state from a theoretical perspective, the spin density surfaces of **DB-1-o** and **DB-1-c** were calculated with DFT method (Figure 6). For **DB-1-o**, the spin density surface is exclusively localized on the iodo-Bodipy moiety, and the open-ring DTE does not contribute to the spin density surface. Thus, the DFT calculation indicates that the T_1 state of **DB-1-o** is localized on the iodo-Bodipy moiety, which is in agreement with the nanosecond time-resolved transient absorption spectroscopy (Figure 4). For **DB-1-c**, similar results were observed. Thus, the lowest-lying triplet state of **DB-1-c** is tentatively assigned to be localized on the iodo-Bodipy moiety, which is also in agreement with the nanosecond time-resolved transient absorption spectra (Figure 5).

dx.doi.org/10.1021/jo5018662 | J. Org. Chem. 2014, 79, 10855−10866

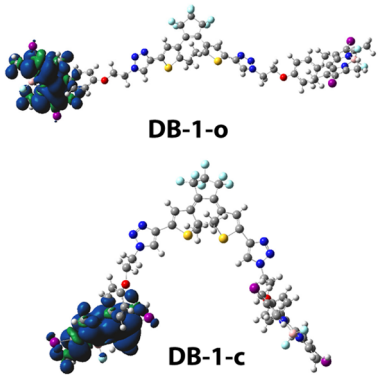

Figure 6. Isosurfaces of spin density of compounds **DB-1-o** and **DB-1-c**, based on optimized triplet state geometries. CH_2Cl_2 was used as solvents in the calculations. Calculation was performed at CAM-B3LYP/6-31G(d)/genecp level with Gaussian 09W.

2.6. Photoswitching of the $^1O_2$ Photosensitizing Ability. To study of the triplet excited-state photoswitching in applications, the $^1O_2$ photosensitizing effects with the **DB-1-o** and the **DB-1-c** were compared (Figure 7). Recently, the $^1O_2$ photosensitizing ability of Zn(II) porphyrin complexes was photoswitched with DTE derivatives.[47a] However, photoswitching of the photosensitizing was never studied with a chromophore dyad or triad, that is, with molecular assemblies based on covalent bond connections. It is well-known that triplet photosensitizer can sensitize $^1O_2$ in the presence of dioxygen (O_2) upon photoexcitation.[2] 1,3-Diphenylisobenzofuran (DPBF) was used as the $^1O_2$ scavenger. The production of $^1O_2$ can be followed by monitoring the absorbance changes at 414 nm.[59−61] We found that the **DB-1-o** is more efficient to produce $^1O_2$ than **DB-1-c** (Figure 7a). The spectral changes of $^1O_2$ photosensitizing are clearly shown in Figure 7b and c. The $^1O_2$ quantum yields (Φ_Δ) of **DB-1-o** and **DB-1-c** were determined as 87.6% and 36.9%, respectively. These results demonstrated that the photoswitching of the triplet excited state of the triad **DB-1** can be transduced. The application of triplet excited-state photoswitching will be promising in areas such as spatially or temporally resolved photodynamic therapy, or molecular devices.

2.7. Photophysical Processes of the Triads upon Photoexcitation. On the basis of the experimental results obtained with the steady-state and the time-resolved spectroscopy, the photophysical processes of **DB-1** upon photoexcitation were summarized in Scheme 2. For **DB-1-o**, selective excitation into the DTE-o moiety at 254 nm will lead to ultrafast DTE-o → DTE-c photocyclization (a few picoseconds),[19,38] which is much faster than the RET to Bodipy moiety (the spectral overlap between the DTE and Bodipy is poor). Thus, the DTE-o → DTE-c process is not perturbed in triad **DB-1** as compared to that of **D-1**. This point was proved by the comparison of the photocyclization of **DB-1** and **D-1** (Supporting Information Figure S24).

Upon selective photoexcitation into the 2,6-diiodoBodipy part in **DB-1-o**, however, intersystem crossing (ISC) will take place to give the triplet excited state. The T_1 state energy level of the DTE-o moiety is higher than that of diiodoBodipy;[19] thus the triplet excited state of diiodoBodipy was not perturbed. This postulation was supported by the similar triplet excited states of **DB-1-o** and **B-0** (Figure 4).

For the **DB-1-c**, however, the relative singlet/triplet excited-state energy levels changed as compared to that in **DB-1-o**; thus the photophysical properties were switched. First, the ISC of the 2,6-diiodoBodipy moiety will compete with the RET to DTE-c moiety, as demonstrated by the enhanced **DTE-c → DTE-o** photoreversion upon excitation into the diiodoBodipy moiety at 535 nm, where the absorption is much stronger than that at 600 nm, and the quenching of the residual fluorescence of the diiodoBodipy moiety. Furthermore, we found that the lifetime of the triplet excited state of **DB-1-c** (40.9 μs), which is localized on the diiodoBodipy part, is much shorter than **DB-1-o** (105.1 μs) or **B-0** (106.4 μs). Thus, it is plausible that a fast decaying triplet excited state, most probably the ^{3}DTE-c state, lies closely to the triplet state of diiodoBodipy moiety. Previously, it was proposed that the ^{3}DTE-c state has a lifetime shorter than 10 ns.[19] Thus, the triplet excited-state lifetime of the Bodipy moiety in **DB-1-c** (40.9 μs) is much shorter than that in **DB-1-o** (105.1 μs). Both the ^{1}DTE-c and the ^{3}DTE-c can lead to a ring-opening reaction.[44] Thus, similar DTE-c → DTE-o kinetics were observed for **DB-1-c** and **DB-2-c**.

2.8. Photoswitched Triplet−Triplet Annihilation Upconversion. Previously, DTE was used for modulation of the fluorescence of organic chromophores,[38,39c,51] the triplet state and phosphorescence of transition metal complexes,[19a,b,43,52] or more recently switching of the singlet oxygen ($^1O_2$) production of porphyrin complexes.[47a] Recently, we reported the first example of photoswitching TTA upconversion with two DTE derivatives in a mixture of the components.[47b] However, photoswitching of the TTA upconversion with an inherently photoswitchable triplet photosensitizer was never reported.[47b] This photoswitchable TTA upconversion protocol is more promising for practical applications. Thus, the photoswitching TTA upconversion with **DB-1** was studied.

For **DB-1**, we demonstrated that the triplet state feature of **DTE-1**, in the aspect of either triplet state lifetime (τ_T) or

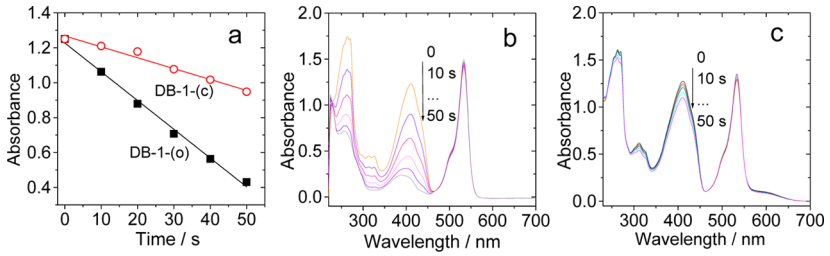

Figure 7. (a) Comparison of singlet oxygen ($^1O_2$) generation of **DB-1-o** and **DB-1-c**. Deeper slop indicates more efficient $^1O_2$ photosensitizing ability. The absorbance decrease traces of DPBF at 414 nm with increasing photoirradiation time in the presence of **DB-1-o** or **DB-1-c** (λ_{ex} = 500 nm). UV−vis absorption spectra of the mixture of (b) **DB-1-o**/DPBF and (c) **DB-1-c**/DPBF. Photoirradiation at λ_{ex} = 535 nm (0.8−1.0 W/m^2) in dichloromethane, c = 1.0 × 10^{-5} M, 20 °C.

dx.doi.org/10.1021/jo5018662 | J. Org. Chem. 2014, 79, 10855−10866

Scheme 2. Simplified Jablonski Diagram Illustrating the Photophysical Processes Involved in (a) DB-1-o and (b) DB-1-c[a]

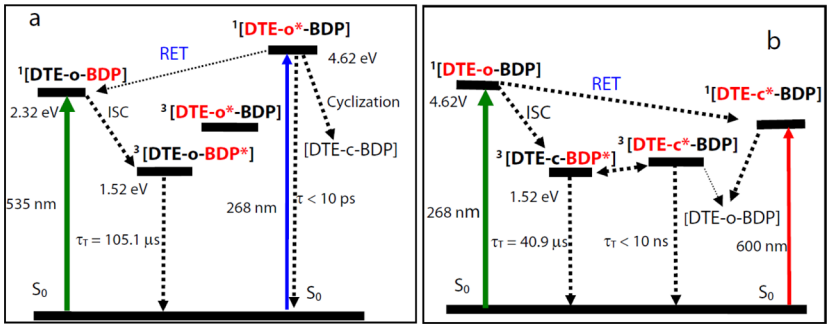

[a][DTE-o-BDP] stands for **DB-1-o**. The component at the excited state was designated with red color and an asterisk. The number of the superscript designated either the singlet or the triplet excited state.

triplet state quantum yields (Φ_T, evaluated by the singlet oxygen quantum yield Φ_Δ), can be substantially modulated upon photoirradiation. Therefore, we investigated the photomodulation of TTA upconversion, with **DB-1** as the triplet photosensitizer and perylene as the triplet acceptor (Figure 8).

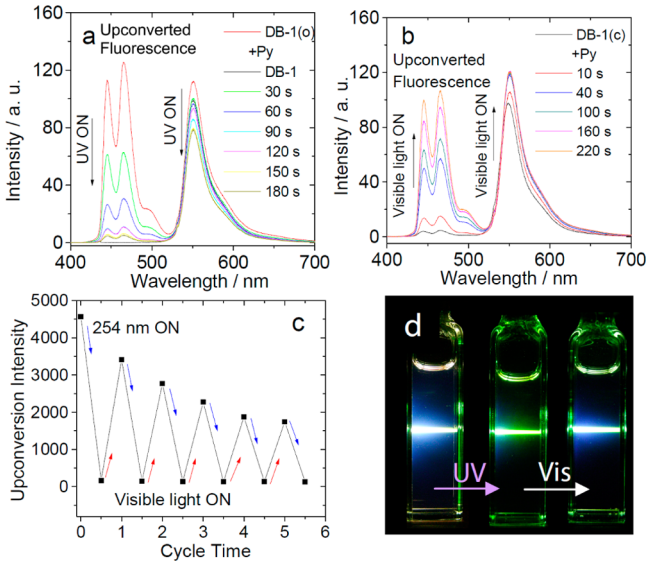

Figure 8. Photoswitching of the TTA UC with **DB-1** as photosensitizer and perylene as acceptor. (a) Upconversion was observed in the presence of open-form **DB-1** but was switched off by irradiation of the mixture at 254 nm. (b) Recovery of the TTA UC, upon irradiation by visible light at >400 nm. (c) The reversibility of the photoswitching of TTA UC with **DB-1** upon alternative UV and visible light irradiation. (d) The photographs of the photoswitching of TTA UC with alternative UV and visible light irradiation. Excited with 532 nm continuous laser (power density: 24.5 mW cm^{-2}), c[**DB-1**] = 1.0 × 10^{-5} M, c[Py] = 1.0 × 10^{-4} M, in deaerated CH_3CN, 20 °C.

For **DB-1-o**, TTA upconversion was observed upon 532 nm excitation (Figure 8a). The upconversion quantum yield is 11.6%. This is in full agreement with the results obtained by the nanosecond transient absorption spectra and the singlet oxygen photosensitizing experiments. Upon 254 nm photoirradiation of the mixed solution, however, the upconversion emission intensity decreased. The upconversion quantum yields decreased to 0.67% at the photostationary state. This decreased upconversion efficiency is most likely due to the reduced triplet state lifetime and the triplet yield in **DB-1-c** as compared to that in **DB-1-o**. Interestingly, the fluorescence emission intensity of **DB-1** at 553 nm was also modulated along with the modulation of the TTA upconversion. The quenching of the fluorescence of **DB-1** at 553 nm is due to the RET effect, as confirmed by the steady-state fluorescence study (Supporting Information Figure S26), which is different from a previous study.[47b] Such a dual photoswitching ability is more promising for application because the OFF−ON emission intensity contrast can be improved.

The photoswitching of the TTA upconversion is reversible. The TTA upconversion intensity was recovered upon visible light irradiation (Figure 8b). This is in agreement with the recovered **DB-1-o** species in the solution. We demonstrated that the TTA upconversion can be switched for more than five times, with only minor loss of the upconversion intensity (Figure 8c). This result is similar to a recent study with mixture of the DTE and the TTA upconversion system.[47b] Photoswitched TTA upconversion will offer unprecedented temporal and spatial resolution for luminescence bioimaging or photodynamic therapy studies.[51,62−64]

2.9. Conclusion. Dithienylethene (DTE)-2,6-diiodoBodipy triad was prepared, with the aim to photoswitch the triplet excited state of organic chromophores. The molecular designing rationale is to perturb the intersystem crossing (ISC) of the 2,6-diiodoBodipy moiety with the photoactivated intramolecular resonance energy transfer (RET), with the closed-ring form of DTE as singlet energy acceptor and 2,6-diiodoBodipy moiety as the singlet energy donor. To the best of our knowledge, this is the first time that a covalently linked organic triplet photosensitizer and DTE photoswitch unit were studied. The photophysical properties of the triad were studied with steady-state and time-resolved transient difference absorption spectroscopy. The open-ring form of DTE (DTE-o, shows no absorption band in visible spectra region) can be reversibly photoswitched to the cyclic structure with 254 nm irradiation, DTE-c, which shows an absorption band at 600 nm; as a result, the residual fluorescence of the 2,6-diiodoBodipy moiety was quenched, and the lifetime of the triplet state of the DTE-o-Bodipy was being greatly reduced from 105.1 to 40.9 μs. Furthermore, the photoreversion was greatly accelerated upon selective photoexcitation into the Bodipy absorption band at 535 nm as compared to that of photoexcitation into the DTE-c moiety (at 600 nm). We observed that the singlet oxygen quantum yield (Φ_Δ) can be reduced from 87.6% to 36.9% upon photoswitching. Furthermore, the photoswitching of the triplet excited state was used to switch the triplet−triplet annihilation upconversion. The study on the photoswitching of the triplet excited state of organic chromophores is rarely reported, and

dx.doi.org/10.1021/jo5018662 | J. Org. Chem. 2014, 79, 10855−10866

these studies will be useful for exploration of the triplet excited-state photophysics of organic chromophore, photoresponsive molecular devices, external stimuli-activatable photodynamic therapy, etc.

3. EXPERIMENTAL SECTION

3.1. General Methods. All of the chemicals used in the synthesss are analytically pure and were used as received. Solvents were dried and distilled before use for synthesis. Luminescence lifetimes were measured on a OB 920 fluorescence/phosphorescence lifetime spectrofluorometer (Edinburgh Instruments, U.K.). Compounds **1**,[15b] **2**,[15b] **3**,[15b] **5**,[34c] and **6**[34c] were reported previously. The molecular characterization data were presented in the Supporting Information.

3.2. Synthesis of 1. [15b] The mixture of *p*-hydroxybenzaldehyde (2.44 g, 20 mmol) and K_2CO_3 (5.53 g, 40 mmol) in EtOH (30 mL) was heated at 70 °C for 30 min, and then 1,2-dibromoethane (7.43 g, 40 mmol) was added. The mixture was stirred and refluxed for 6 h. The reaction mixture was concentrated under reduced pressure to give a yellow solid. The solid then was dissolved in CH_2Cl_2, dried over anhydrous Na_2SO_4, and filtrated. The solvent was removed under reduced pressure. The crude product was purified by column chromatography (silica gel, CH_2Cl_2:PE = 1:2, v/v) to give compound **1** as a white solid (2.50 g, yield: 60.0%). ^{1}H NMR (400 MHz, $CDCl_3$): δ 9.90 (s, 1H, J = 8.0 Hz), 7.86 (d, 2H, J = 8.0 Hz), 7.03 (d, 2H, J = 8.0 Hz), 4.38 (t, 2H, J = 4.0 Hz, J = 8.0 Hz), 3.67 (t, 2H, J = 4.0 Hz, J = 8.0 Hz). HRMS: m/z calcd ($[C_9H_9BrO_2]^+$), m/z = 227.9786, found m/z = 227.9777.

3.3. Synthesis of 2. [15b] Compound **1** (2.50 g, 11.0 mmol) and NaN_3 (0.90 g, 12.0 mmol) were dissolved in DMF (5 mL), and then the mixture was refluxed with stirring for 2 h. The solution was cooled to room temperature (RT) and diluted with CH_2Cl_2, washed with water several times, and the organic layer was dried over anhydrous Na_2SO_4. The mixture was filtrated, and the solvent was removed under reduced pressure to give a yellow oil (1.68 g, yield: 80.4%). ^{1}H NMR (400 MHz, $CDCl_3$): δ 9.89 (s, 1H), 7.86 (d, 2H, J = 8.0 Hz), 7.04 (d, 2H, J = 8.0 Hz), 4.23 (t, 2H, J = 4.0 Hz), 3.65 (t, 2H, J = 4.0 Hz). MALDI-HRMS: m/z calcd ($[C_9H_9N_3O_2 + H]^+$) m/z = 192.0766, found m/z = 192.0763.

3.4. Synthesis of 3. [15b] Under N_2 atmosphere, a mixture of compound **2** (1.91 g, 10 mmol) and 2,4-dimethylpyrrole (1.88 g, 20 mmol) in dry CH_2Cl_2 (250 mL) was stirred at rt. TFA (0.1 mL) then was added into the mixture by syringe, and the mixture was stirred at rt overnight. 2,3-Dichloro-5,6-dicyanobenzoquinone (DDQ. 1.13 g, 5 mmol) was dissolved in dry DCM (30 mL), and the solution was added into the mixture in one portion, and then the mixture was stirred at rt for 7 h. Triethylamine (10 mL) was added dropwise to the mixture with cooling by ice bath. The reaction mixture was stirred for another 0.5 h. $BF_3{\cdot}Et_2O$ (10 mL) then was added dropwise into the mixture. The reaction mixture was stirred overnight. The solution was concentrated under reduced pressure, and water (200 mL) was added. The mixture was stirred for 24 h. The solution then was extracted with CH_2Cl_2 (3 × 100 mL), and the organic layer was dried over anhydrous Na_2SO_4. The solvent was evaporated under reduced pressure. The crude product was purified by column chromatography (silica gel, CH_2Cl_2:hexane = 1:1, v/v) to give compound **3** as a red solid (300 mg, yield: 7.5%). ^{1}H NMR (400 MHz, $CDCl_3$): δ 7.21 (d, 2 H, J = 12.0 Hz), 7.05 (d, 2H, J = 12.0 Hz), 5.98 (s, 2H), 4.21 (t, 2H, J = 4.0 Hz), 3.67 (t, 2H, J = 4.0 Hz), 2.55 (s, 6H), 1.43 (s, 6H). Mp, 146−148 °C. MALDI-HRMS: m/z calcd ($[C_{21}H_{22}N_5OBF_2]^+$), m/z = 409.1885, found m/z = 409.1859.

3.5. Synthesis of 4. To a mixture of *N*-bromosuccinimide (7.25 g, 40.7 mmol) and AcOH (50 mL) was added dropwise a solution of 2-methylthiophene (2 g, 20.4 mmol) in AcOH (20 mL). The mixture was stirred at rt for 12 h. The mixture was poured into a mixture of petroleum ether (100 mL) and water (100 mL). The organic layer was washed with 1 M sodium hydroxide and brine successively, and was dried over anhydrous Na_2SO_4. The solvent was removed under reduced pressure to give the product as 4.67 g of yellow oil (yield: 90.3%). The product was used for the next reaction without further purification.

3.6. Synthesis of 5. [34c] Under Ar atmosphere, 3,5-dibromo-2-methylthiophene (0.76 g, 3.0 mmol) was dissolved in Et_3N (100 mL), and then $Pd(PPh_3)_4$ (93.0 mg, 3% mmol), CuI (26.6 mg, 5% mmol), and trimethylsilylacetylene (TMSA) (0.4 mL, 2.8 mmol) were added successively. The mixture was stirred at 45 °C for 7 h. The solvent was evaporated under reduced pressure. The crude product was purified by column chromatography to give a yellow solid (350 mg, yield: 45.5% from TMSA). ^{1}H NMR (400 MHz, $CDCl_3$): δ 7.02 (s, 1H), 2.36 (s, 3H), 0.23 (s, 9H). TOF HRMS EI$^+$: calcd for ($[C_{10}H_{13}SiSBr]^+$), m/z = 271.9691, found m/z = 271.9694.

3.7. Synthesis of 6. [34c] Under Ar atmosphere, a solution of compound **5** (479 mg, 1.76 mmol) in dry ether (25 mL) was cooled to −78 °C. *n*-Butyllithium (1.6 M in hexane, 2.2 mL, 3.5 mmol) was added into the resulting solution, and the temperature was kept at −78 °C for 2 h. Perfluorocyclopentene (0.1 mL, 0.8 mmol) then was added with a syringe quickly, and the mixture was stirred for another 2 h at −78 °C. The solution then was warmed to room temperature, and the mixture was stirred for 2 h and then diluted with diethyl ether. The mixture was washed with dilute hydrochloric acid solution (1%, 3 × 30 mL), extracted with diethyl ether (3 × 50 mL), and dried over anhydrous Na_2SO_4. The filtrate was evaporated under reduced pressure, and the crude product was purified by column chromatography (silica gel, PE as the eluent) to give a bluish white solid (250 mg, yield: 30.0%). ^{1}H NMR (400 MHz, $CDCl_3$): δ 7.19 (s, 2H), 1.88 (s, 6H), 0.24 (s, 18H). MALDI-HRMS: m/z calcd ($[C_{25}H_{26}F_6S_2Si_2]^+$), m/z = 560.0919, found m/z = 560.0890.

3.8. Synthesis of B-0. To a solution of compound **3** (200 mg, 0.49 mmol) in anhydrous CH_2Cl_2 (25 mL) was added *N*-iodosuccinimide (NIS, 558 mg, 2.48 mmol). The mixture was stirred at 30 °C overnight. The reaction mixture was concentrated under vacuum, and the residue was purified by column chromatography (silica gel, hexane/CH_2Cl_2, 2:1, v/v). The red band was collected, and the solvent was removed under reduced pressure to give the product as a red solid (280.0 mg, yield: 90.4%). Mp 174−176 °C. ^{1}H NMR (400 MHz, $CDCl_3$): δ 7.18 (d, 2H, J = 8.0 Hz), 7.08 (d, 2H, J = 8.0 Hz), 4.23 (t, 2H, J = 4.0 Hz), 3.69 (t, 2H, J = 4.0 Hz), 2.65 (s, 6H), 1.45 (s, 6H). MALDI-HRMS: calcd ($[C_{21}H_{20}N_5OBF_2I_2]^+$), m/z = 660.9819, found m/z = 660.9866.

3.9. Synthesis of D-1. To a solution of **6** (250 mg, 0.45 mmol) in methanol/THF (4:1, v:v) was added NaOH (180 mg, 4.5 mmol), and the mixture was stirred at room temperature for 45 min. The resulting solution was extracted with dichloromethane. The organic layer was washed with water, and dried over anhydrous Na_2SO_4. The solvent was evaporated under reduced pressure. The crude product was purified by chromatography to give a bluish white solid (130 mg, yield: 70.0%). Mp, 94−96 °C. ^{1}H NMR (400 MHz, $CDCl_3$): δ 7.24 (s, 2H), 3.36 (s, 2H), 1.89 (s, 6H). TOF HRMS EI$^+$: calcd ($[C_{19}H_{10}F_6S_2]^+$), m/z = 416.0128, found m/z = 416.0122.

3.10. Synthesis of DB-1. Under Ar atmosphere, **D-1** (20.0 mg, 0.05 mmol) and **B-0** (66 mg, 0.1 mmol) were dissolved in mixed solvent $CHCl_3$/MeOH/H_2O (8 mL, 6:1:1, v/v). $CuSO_4{\cdot}5H_2O$ (7.5 mg) and sodium ascorbate (11.5 mg) then were added, respectively. The mixture was stirred at 25 °C for 48 h. The reaction mixture then was washed with water and extracted with CH_2Cl_2 (3 × 50 mL). The organic layer was dried over anhydrous Na_2SO_4 and evaporated under reduced pressure. The crude product was purified by column chromatography (silica gel, CH_2Cl_2:CH_3OH = 100:1, v/v) to give a red solid (40.0 mg, yield: 46.6%). Mp, 152−154 °C. ^{1}H NMR (400 MHz, $CDCl_3$): δ 7.90 (s, 2H), 7.37 (s, 2H), 7.17 (d, 4H, J = 12.0 Hz), 7.04 (d, 4H, J = 12.0 Hz), 4.84 (t, 4H, J = 4.0 Hz), 4.49 (t, 4H, J = 4.0 Hz), 2.63 (s, 12H), 1.98 (s, 6H), 1.40 (s, 12H). ^{13}C NMR (100 MHz, $CDCl_3$): 158.71, 156.82, 145.23, 141.80, 140.88, 131.59, 131.13, 129.43, 127.96, 125.42, 123.50, 120.46, 115.40, 85.71, 66.38, 49.60, 33.69, 31.93, 24.73, 17.24, 16.04, 14.60. MALDI-HRMS: calcd ($[C_{61}H_{50}N_{10}O_2B_2F_{10}I_4S_2]^-$), m/z = 1737.9765, found m/z = 1737.9762.

3.11. Synthesis of DB-2. Under Ar atmosphere, compounds **3** (20.0 mg, 0.05 mmol) and **D-1** (40 mg, 0.1 mmol) were dissolved in

dx.doi.org/10.1021/jo5018662 | J. Org. Chem. 2014, 79, 10855−10866

the mixed solvent $CHCl_3$/MeOH/H_2O (8 mL, 6:1:1, v/v), and then $CuSO_4 \cdot 5H_2O$ (7.5 mg) and sodium ascorbate (11.5 mg) were added, respectively. The mixture was stirred at rt for 48 h. The reaction mixture then was washed with water and extracted with CH_2Cl_2. The organic layer was dried over anhydrous Na_2SO_4. The solvent was evaporated under reduced pressure, and the crude product was purified by column chromatography (silica gel, CH_2Cl_2:CH_3OH = 100:1, v/v) to give an orange solid (45.0 mg, yield: 73.4%). Mp, 142−144 °C. ^{1}H NMR (400 MHz, $CDCl_3$): δ 7.91 (s, 2H), 7.37 (s, 2H), 7.20 (d, 4H, J = 8.0 Hz), 7.01 (d, 4H, J = 8.0 Hz), 5.98 (s, 4H), 4.84 (t, 4H, J = 4.0 Hz), 4.47 (t, 4H, J = 4.0 Hz), 2.55 (s, 12H), 1.98 (s, 6H), 1.40 (s, 12H). ^{13}C NMR (100 MHz, $CDCl_3$): 158.41, 155.38, 143.15, 142.16, 141.86, 141.31, 131.80, 131.27, 129.61, 128.34, 125.48, 123.53, 121.33, 120.63, 115.18, 66.41, 50.12, 33.99, 32.05, 24.85, 22.82, 14.77. MALDI-HRMS: calcd ($[C_{61}H_{53}N_{10}O_2S_2B_2F_{10} - H^+]^-$), m/z = 1233.3821; found m/z = 1233.3868.

3.12. Cyclic Voltammetry (CV). The CV measurements were performed using a CHI610D Electrochemical workstation (Shanghai, China). Cyclic voltammograms were recorded at scan rates of 50 mV/s. A three-electrodes cell was used. Electrochemical measurements were performed at rt using 0.1 M tetrabutylammonium hexafluorophosphate (TBAP) as supporting electrolyte, after purging with N_2. The working electrode was a glassy carbon electrode, and the counter electrode was platinum electrode. A nonaqueous Ag/$AgNO_3$ (0.1 M in CH_3CN) reference electrode was contained in a separate compartment connected to the solution via frit. CH_3CN was used as the solvent. Ferrocene was added as the internal reference. The close-form DTE derivatives were obtained by photoirradiation of open-form solution with 254 nm UV lamp (0.7−1.0 W/m^2) for 1−1.5 h.

3.13. Nanosecond Time-Resolved Transient Difference Absorption Spectra. The nanosecond time-resolved transient absorption spectra were detected by laser flash photolysis spectrometer (LP920, Edinburgh Instruments, UK) and recorded on a Tektronix TDS 3012B oscilloscope. The lifetime values (by monitoring the decay trace of the transients) were obtained with the LP900 software. All samples in flash photolysis experiments were deaerated with argon for ca. 15 min before measurement, and the gas flow was maintained during the measurement. PMT detector or ICCD detector (Andor DH720) was used.

3.14. Triplet−Triplet Annihilation Upconversions. A diode pumped solid-state (DPSS) continuous laser (532 nm) was used for the upconversion. The diameter of the 532 nm laser spot was ca. 3 mm. The power of the laser beam was measured with a VLP-2000 pyroelectric power meter. The samples were purged with N_2 or Ar for at least 15 min before measurement. For the upconversion experiments, the mixed solution of **DB-1** (triplet photosensitizer) and perylene (triplet energy acceptor) was degassed for at least 15 min with N_2. The solution then was irradiated by a 254 nm UV lamp or visible light (λ > 400 nm) for different time intervals. The upconverted fluorescence of perylene was observed with a RF5301 spectrofluorometer. To suppress the laser scattering, a black box with a small hole was put behind the fluorescent cuvette to damp the laser beam (the small hole as the entrance of the laser into the black box).

3.15. DFT Calculations. The density functional theory (DFT) calculations were used for optimization of the ground-state geometries of both singlet states and triplet states. The energy level of the T_1 state (energy gap between the S_0 state and T_1 state) was approximated with time-dependent DFT (TDDFT), based on the optimized singlet ground-state geometries (S_0 state). All of the calculations were performed with Gaussian 09W.[65]

■ ASSOCIATED CONTENT

Supporting Information

Free energy calculations, molecular structure characterization data (NMR, HRMS spectra) and emission spectra, cyclovoltammetric graph, and tables of atom coordinates. This material is available free of charge via the Internet at http://pubs.acs.org.

■ AUTHOR INFORMATION

Corresponding Authors

*E-mail: zhaojzh@dlut.edu.cn. Web: http://finechem2.dlut.edu.cn/photochem.

*E-mail: xwli@dicp.ac.cn.

Notes

The authors declare no competing financial interest.

■ ACKNOWLEDGMENTS

We thank the NSFC (20972024, 21273028, 21421005, and 21473020), the Royal Society (UK) and NSFC (China-UK Cost-Share Science Networks, 21011130154), the Ministry of Education (NCET-08-0077 and SRFDP-20120041130005) Program for Changjiang Scholars and Innovative Research Team in University [IRT_13R06], the Fundamental Research Funds for the Central Universities (DUT14ZD226), and Dalian University of Technology (DUT2013TB07) for financial support.

■ REFERENCES

(1) Wang, W.; Wang, F.; Wang, H.; Tung, C.; Wu, Li. *Dalton Trans.* **2012**, *41*, 2420−2426.

(2) Kamkaew, A.; Lim, S.; Lee, H.; Kiew, L.; Chung, L.; Burgess, K. *Chem. Soc. Rev.* **2013**, *42*, 77−88.

(3) Awuah, S.; You, Y. *RSC Adv.* **2012**, *2*, 11169−11183.

(4) Zhao, J.; Wu, W.; Sun, J.; Guo, S. *Chem. Soc. Rev.* **2013**, *42*, 5323−5351.

(5) Gärtner, F.; Cozzula, D.; Losse, S.; Boddien, A.; Anilkumar, G.; Junge, H.; Schulz, T.; Marquet, N.; Spannenberg, A.; Gladiali, S.; Beller, M. *Chem.—Eur. J.* **2011**, *17*, 6998−7006.

(6) (a) Goldsmith, J.; Hudson, W. R.; Lowry, M. S.; Anderson, T. H.; Bernhard, S. *J. Am. Chem. Soc.* **2005**, *127*, 7502−7510. (b) Junge, H.; Marquet, N.; Kammer, A.; Denurra, S.; Bauer, M.; Wohlrab, S.; Gärtner, F.; Pohl, M.; Spannenberg, A.; Gladiali, S.; Beller, M. *Chem.—Eur. J.* **2012**, *18*, 12749−12758. (c) Lalevée, J.; Peter, M.; Dumur, F.; Gigmes, D.; Blanchard, N.; Tehfe, M.-A.; Morlet-Savary, F.; Fouassier, J. P. *Chem.—Eur. J.* **2011**, *17*, 15027−15031. (d) Zhou, H.; Lu, P.; Gu, X.; Li, P. *Org. Lett.* **2013**, *15*, 5646−5649.

(7) (a) Feng, Y.; Cheng, J.; Zhou, L.; Zhou, X.; Xiang, H. *Analyst* **2012**, *137*, 4885−4901. (b) Xiang, H.; Zhou, L.; Feng, Y.; Cheng, J.; Wu, D.; Zhou, X. *Inorg. Chem.* **2012**, *51*, 5208−5212. (c) Guo, H.; Ji, S.; Wu, W.; Wu, W.; Shao, J.; Zhao, J. *Analyst* **2010**, *135*, 2832−2840. (d) Wu, W.; Wu, W.; Ji, S.; Guo, H.; Song, P.; Han, K.; Chi, L.; Shao, J.; Zhao, J. *J. Mater. Chem.* **2010**, *20*, 9775−9786. (e) Ji, S.; Wu, W.; Wu, W.; Song, P.; Han, K.; Wang, Z.; Liu, S.; Guo, H.; Zhao, J. *J. Mater. Chem.* **2010**, *20*, 1953−1963.

(8) Erbas-Cakmak, S.; Akkaya, E. *Angew. Chem., Int. Ed.* **2013**, *52*, 11364−11368.

(9) Erbas-Cakmak, S.; Altan Bozdemir, O.; Cakmaka, Y.; Akkaya, E. *Chem. Sci.* **2013**, *4*, 858−862.

(10) McDonnell, S.; Hall, M.; Allen, L.; Byrne, A.; Gallagher, W.; O'Shea, D. *J. Am. Chem. Soc.* **2005**, *127*, 16360−16361.

(11) Yogo, T.; Urano, Y.; Ishitsuka, Y.; Maniwa, F.; Nagano, T. *J. Am. Chem. Soc.* **2005**, *127*, 12162−12163.

(12) (a) Schmitt, F.; Freudenreich, J.; Barry, N.; Juillerat-Jeanneret, L.; Süss-Fink, G.; Therrien, B. *J. Am. Chem. Soc.* **2012**, *134*, 754−757. (b) Gao, Y.; Ou, Z.; Chen, J.; Yang, G.; Wang, X.; Zhang, B.; Jin, M.; Liu, L. *New J. Chem.* **2008**, *32*, 1555−1560.

(13) Tian, J.; Ding, L.; Xu, H.; Shen, Z.; Ju, H.; Jia, L.; Bao, L.; Yu, J. *J. Am. Chem. Soc.* **2013**, *135*, 18850−18858.

(14) Singh-Rachford, T.; Castellano, F. *Coord. Chem. Rev.* **2010**, *254*, 2560−2573.

(15) (a) Zhao, J.; Ji, S.; Guo, H. *RSC Adv.* **2011**, *1*, 937−950. (b) Zhang, C.; Zhao, J.; Wu, S.; Wang, Z.; Wu, W.; Ma, J.; Guo, S.; Huang, L. *J. Am. Chem. Soc.* **2013**, *135*, 10566−10578. (c) Ji, S.; Wu, W.; Wu, W.; Guo, H.; Zhao, J. *Angew. Chem., Int. Ed.* **2011**, *50*, 1626−

1629. (d) Ji, S.; Guo, H.; Wu, W.; Wu, W.; Zhao, J. *Angew. Chem., Int. Ed.* **2011**, *50*, 8283−8286.
(16) Monguzzi, A.; Tubino, R.; Hoseinkhani, S.; Campioneb, M.; Meinardib, F. *Phys. Chem. Chem. Phys.* **2012**, *14*, 4322−4332.
(17) (a) Ceroni, P. *Chem.—Eur. J.* **2011**, *17*, 9560−9564. (b) Simon, Y.; Weder, C. *J. Mater. Chem.* **2012**, *22*, 20817−20830.
(18) (a) Peng, J.; Jiang, X.; Guo, X.; Zhao, D.; Ma, Y. *Chem. Commun.* **2014**, *50*, 7828−7830. (b) Wang, B.; Sun, B.; Wang, X.; Ye, C.; Ding, P.; Liang, Z.; Chen, Z.; Tao, X.; Wu, L. *J. Phys. Chem. C* **2014**, *118*, 1417−1425. (c) Borisov, S. M.; Saf, R.; Fischer, R.; Klimant, I. *Inorg. Chem.* **2013**, *52*, 1206−1216.
(19) (a) Jukes, R.; Adamo, V.; Hartl, F.; Belser, P.; De Cola, L. *Inorg. Chem.* **2004**, *43*, 2779−2792. (b) Indelli, M. T.; Carli, S.; Ghirotti, M.; Chiorboli, C.; Ravaglia, M.; Garavelli, M.; Scandola, F. *J. Am. Chem. Soc.* **2008**, *130*, 7286−7299.
(20) Chan, J.; Lam, W.; Wong, H.; Zhu, N.; Wong, W.; Yam, V. *J. Am. Chem. Soc.* **2011**, *133*, 12690−12705.
(21) Silva, A.; Gunaratne, H.; Gunnlaugsson, T.; Huxley, A.; McCoy, C.; Rademacher, J.; Rice, T. *Chem. Rev.* **1997**, *97*, 1515−1566.
(22) (a) Chen, X.; Zhou, Y.; Peng, X.; Yoon, J. *Chem. Soc. Rev.* **2010**, *39*, 2120−2135. (b) Pan, H.; Fu, G.-L.; Zhao, Y.-H.; Zhao, C.-H. *Org. Lett.* **2011**, *13*, 4830−4833. (c) Shen, X. Y.; Wang, Y. J.; Zhao, E.; Yuan, W. Z.; Liu, Y.; Lu, P.; Qin, A.; Ma, Y.; Sun, J. Z.; Tang, B. Z. *J. Phys. Chem. C* **2013**, *117*, 7334−7347. (d) Apak, R.; Cekic, S. D.; Cetinkaya, A.; Filik, H.; Hayvali, M.; Kili, E. *J. Agric. Food Chem.* **2012**, *60*, 2769−2777.
(23) Ziessel, R.; Harrimanb, A. *Chem. Commun.* **2011**, *47*, 611−631.
(24) Bozdemir, O.; Erbas-Cakmak, S.; Oner Ekiz, O.; Dana, A.; Akkaya, E. *Angew. Chem., Int. Ed.* **2011**, *50*, 10907−10912.
(25) Fan, J.; Hu, M.; Zhan, P.; Peng, X. *Chem. Soc. Rev.* **2013**, *42*, 29−43.
(26) Bandichhor, R.; Petrescu, A.; Vespa, A.; Kier, A.; Schroeder, F.; Burgess, K. *J. Am. Chem. Soc.* **2006**, *128*, 10688−10689.
(27) Peng, X.; Du, J.; Fan, J.; Wang, J.; Wu, Y.; Zhao, J.; Sun, S.; Xu, T. *J. Am. Chem. Soc.* **2007**, *129*, 1500−1501.
(28) (a) Zhang, Q.; Zhu, Z.; Zheng, Y.; Cheng, J.; Zhang, N.; Long, Y.; Zheng, J.; Qian, X.; Yang, Y. *J. Am. Chem. Soc.* **2012**, *134*, 18479−18482. (b) Wu, Y.; Zhu, W. *Chem. Soc. Rev.* **2013**, *42*, 2039−2058.
(29) Cheng, T.; Xu, Y.; Zhang, S.; Zhu, W.; Qian, X.; Duan, L. *J. Am. Chem. Soc.* **2008**, *130*, 16160−16161.
(30) Lakowicz, J. R. *Principles of Fluorescence Spectroscopy*, 2nd ed.; Kluwer Academic: New York, 1999.
(31) Yuan, M.; Yin, X.; Zheng, H.; Ouyang, C.; Zuo, Z.; Liu, H.; Li, Y. *Chem.—Asian J.* **2009**, *4*, 707−713.
(32) El-Khouly, M.; Amin, A.; Zandler, M.; Fukuzumi, S.; D'Souza, F. *Chem.—Eur. J.* **2012**, *18*, 5239−5247.
(33) Guliyev, R.; Coskun, A.; Akkaya, E. *J. Am. Chem. Soc.* **2009**, *131*, 9007−9013.
(34) (a) Takami, S.; Kuroki, L.; Irie, M. *J. Am. Chem. Soc.* **2007**, *129*, 7319−7326. (b) Mori, K.; Ishibashi, Y.; Matsuda, H.; Ito, S.; Nagasawa, Y.; Nakagawa, H.; Uchida, K.; Yokojima, S.; Nakamura, S.; Irie, M.; Miyasaka, H. *J. Am. Chem. Soc.* **2011**, *133*, 2621−2625. (c) Osuka, A.; Fujikane, D.; Shinmori, H.; Kobatake, S.; Irie, M. *J. Org. Chem.* **2001**, *66*, 3913−3923.
(35) (a) Mierloo, S.; Hadipour, A.; Spijkman, M.; Brande, N.; Ruttens, B.; Kesters, J.; D'Haen, J.; Assche, G.; Leeuw, D.; Aernouts, T.; Manca, J.; Lutsen, L.; Vanderzande, D.; Maes, W. *Chem. Mater.* **2012**, *24*, 587−593. (b) Pu, S.; Tong, Z.; Liu, G.; Wang, R. *J. Mater. Chem. C* **2013**, *1*, 4726−4739. (c) Hu, F.; Huang, J.; Cao, M.; Chen, Z.; Yang, Y.-W.; Liu, S. H.; Yin, J. *Org. Biomol. Chem.* **2014**, *12*, 7712−7720. (d) Lin, Y.; Yuan, J.; Hu, M.; Cheng, J.; Yin, J.; Jin, S.; Liu, S. H. *Organometallics* **2009**, *28*, 6402−6409.
(36) (a) Kozlov, D.; Castellano, F. *J. Phys. Chem. A* **2004**, *108*, 10619−10622. (b) Brayshaw, S.; Schiffers, S.; Stevenson, A.; Teat, S.; Warren, M.; Bennett, R.; Sazanovich, I.; Buckley, A.; Weinstein, J.; Raithby, P. *Chem.—Eur. J.* **2011**, *17*, 4385−4395.
(37) Wu, Y.; Xie, Y.; Zhang, Q.; Tian, H.; Zhu, W.; Li, A. D. Q. *Angew. Chem., Int. Ed.* **2014**, *53*, 2090−2094.
(38) (a) Golovkova, T.; Kozlov, D.; Neckers, D. *J. Org. Chem.* **2005**, *70*, 5545−5549. (b) Giraud, M.; Léaustic, A.; Guillot, R.; Yu, P.; Lacroix, P. G.; Nakatani, K.; Pansuc, R.; Maurel, F. *J. Mater. Chem.* **2007**, *17*, 4414−4425. (c) Spangenberg, A.; Métivier, R.; Yasukuni, R.; Shibata, K.; Brosseau, A.; Grand, J.; Aubard, J.; Yu, P.; Asahiy, T.; Nakatani, K. *Phys. Chem. Chem. Phys.* **2013**, *15*, 9670−9678.
(39) (a) Yildiz, I.; Impellizzeri, S.; Deniz, E.; McCaughan, B.; Callan, J.; Raymo, F. *J. Am. Chem. Soc.* **2011**, *133*, 871−879. (b) Deniz, E.; Ray, S.; Tomasulo, M.; Impellizzeri, S.; Sortino, S.; Raymo, F. *J. Phys. Chem. A* **2010**, *114*, 11567−11575. (c) Kong, L.; Wong, H.-L.; Tam, A. Y.-Y.; Lam, W. H.; Wu, L.; Yam, V. W.-W. *ACS Appl. Mater. Interfaces* **2014**, *6*, 1550−1562. (d) Maisonneuve, S.; Métivier, R.; Yu, P.; Nakatani, K.; Xie, J. *Beilstein J. Org. Chem.* **2014**, *10*, 1471−1481.
(40) Ko, C.; Yam, V. *J. Mater. Chem.* **2010**, *20*, 2063−2070.
(41) Roberts, M.; Nagle, J.; Majewski, M.; Finden, J.; Branda, N.; Wolf, M. *Inorg. Chem.* **2011**, *50*, 4956−4966.
(42) Yam, V.; Ko, C.; Zhu, N. *J. Am. Chem. Soc.* **2004**, *126*, 12734−12735.
(43) Ko, C.; Kwok, W.; Yam, V.; Phillips, D. *Chem.—Eur. J.* **2006**, *12*, 5840−5848.
(44) He, B.; Wenger, O. *Inorg. Chem.* **2012**, *51*, 4335−4342.
(45) Roberts, M.; Carling, C.; Nagle, J.; Branda, N.; Wolf, M. *J. Am. Chem. Soc.* **2009**, *131*, 16644−16645.
(46) (a) Yam, V.; Ko, C.; Wu, L.; Wong, K.; Cheung, K. *Organometallics* **2000**, *19*, 1820−1822. (b) Ko, C.; Wu, L.; Wong, K.; Zhu, N.; Yam, V. *Chem.—Eur. J.* **2004**, *10*, 766−776.
(47) (a) Hou, L.; Zhang, X.; Pijper, T.; Browne, W.; Feringa, B. *J. Am. Chem. Soc.* **2014**, *136*, 910−913. (b) Cui, X.; Zhao, J.; Zhou, Y.; Ma, J.; Zhao, Y. *J. Am. Chem. Soc.* **2014**, *136*, 9256−9259.
(48) Wu, W.; Zhao, J.; Sun, J.; Guo, S. *J. Org. Chem.* **2012**, *77*, 5305−5312.
(49) Sánchez, R. S.; Gras-Charles, R.; Bourdelande, J. L.; Guirado, G.; Hernando, J. *J. Phys. Chem. C* **2012**, *116*, 7164−7172.
(50) Uno, K.; Niikura, H.; Morimoto, M.; Ishibashi, Y.; Miyasaka, H.; Irie, M. *J. Am. Chem. Soc.* **2011**, *133*, 13558−13564.
(51) Zou, Y.; Yi, T.; Xiao, S.; Li, F.; Li, C.; Gao, X.; Wu, J.; Yu, M.; Huang, C. *J. Am. Chem. Soc.* **2008**, *130*, 15750−15751.
(52) Tan, W.; Zhang, Q.; Zhang, J.; Tian, H. *Org. Lett.* **2009**, *11*, 161−164.
(53) Wu, W.; Guo, H.; Wu, W.; Ji, S.; Zhao, J. *J. Org. Chem.* **2011**, *76*, 7056−7064.
(54) (a) Irie, M. *Chem. Rev.* **2000**, *100*, 1685−1716. (b) Apperloo, J.; Martineau, C.; Hal, P.; Roncali, J.; Janssen, R. J. *J. Phys. Chem. A* **2002**, *106*, 21−31. (c) Sabatini, R.; McCormick, T.; Lazarides, T.; Wilson, K.; Eisenberg, R.; McCamant, D. *J. Phys. Chem. Lett.* **2011**, *2*, 223−227.
(55) Rachford, A.; Ziessel, R.; Bura, T.; Retailleau, P.; Castellano, F. *Inorg. Chem.* **2010**, *49*, 3730−3736.
(56) Wu, W.; Zhao, J.; Guo, H.; Sun, J.; Ji, S.; Wang, Z. *Chem.—Eur. J.* **2012**, *18*, 1961−1968.
(57) Wu, W.; Zhao, J.; Sun, J.; Huang, L.; Yi, X. *J. Mater. Chem. C* **2013**, *1*, 705−716.
(58) Sun, J.; Zhong, F.; Yi, X.; Zhao, J. *Inorg. Chem.* **2013**, *52*, 6299−6310.
(59) Takizawa, S.; Aboshi, R.; Murata, S. *Photochem. Photobiol. Sci.* **2011**, *10*, 895−903.
(60) Sun, J.; Zhao, J.; Guo, H.; Wu, W. *Chem. Commun.* **2012**, *48*, 4169−4171.
(61) Adarsh, N.; Shanmugasundaram, M.; Avirah, R.; Ramaiah, D. *Chem.—Eur. J.* **2012**, *18*, 12655−12662.
(62) Liu, Q.; Yang, T.; Feng, W.; Li, F. *J. Am. Chem. Soc.* **2012**, *134*, 5390−5397.
(63) Kang, J.; Reichmanis, E. *Angew. Chem., Int. Ed.* **2012**, *51*, 11841−11844.
(64) Kim, J.-H.; Kim, J.-H. *J. Am. Chem. Soc.* **2012**, *134*, 17478−17481.
(65) Frisch, M. J.; Trucks, G. W.; Schlegel, H. B.; Scuseria, G. E.; Robb, M. A.; Cheeseman, J. R.; Scalmani, G.; Barone, V.; Mennucci, B.; Petersson, G. A.; Nakatsuji, H.; Caricato, M.; Li, X.; Hratchian, H.

P.; Izmaylov, A. F.; Bloino, J.; Zheng, G.; Sonnenberg, J. L.; Hada, M.; Ehara, M.; Toyota, K.; Fukuda, R.; Hasegawa, J.; Ishida, M.; Nakajima, T.; Honda, Y.; Kitao, O.; Nakai, H.; Vreven, T.; Montgomery, J. A., Jr.; Peralta, J. E.; Ogliaro, F.; Bearpark, M.; Heyd, J. J.; Brothers, E.; Kudin, K. N.; Staroverov, V. N.; Kobayashi, R.; Normand, J.; Raghavachari, K.; Rendell, A.; Burant, J. C.; Iyengar, S. S.; Tomasi, J.; Cossi, M.; Rega, N.; Millam, J. M.; Klene, M.; Knox, J. E.; Cross, J. B.; Bakken, V.; Adamo, C.; Jaramillo, J.; Gomperts, R.; Stratmann, R. E.; Yazyev, O.; Austin, A. J.; Cammi, R.; Pomelli, C.; Ochterski, J. W.; Martin, R. L.; Morokuma, K.; Zakrzewski, V. G.; Voth, G. A.; Salvador, P.; Dannenberg, J. J.; Dapprich, S.; Daniels, A. D.; Farkas, Ö.; Foresman, J. B.; Ortiz, J. V.; Cioslowski, J.; Fox, D. J. *Gaussian 09*, revision D.01; Gaussian, Inc.: Wallingford, CT, 2009.